Supporting Information

Fast-Response, Sensitivitive and Low-Powered Chemosensors by Fusing Nanostructured Porous Thin Film and IDEs-Microheater Chip

Zhengfei Dai[†,§], Lei Xu[‡,#,§], Guotao Duan[*,†], Tie Li[*,‡], Hongwen Zhang[†], Yue Li[†], Yi Wang[‡], Yuelin Wang[‡], and Weiping Cai[†]

* Corresponding authors:

duangt@issp.ac.cn (G.D.); tli@mail.sim.ac.cn (T.L.); ylwang@mail.sim.ac.cn; (Y.L.W.)wpcai@issp.ac.cn (W.C).

1. Fabrication of the supporting system of the device (sandwich chip)

The IDEs-microheater chip was fabricated based on classic MEMS processes. (i) A double-side-polished 350μm-thickness N-type <100> oriented silicon wafer with a layer of SiO_2 (200 nm in thickness) thermally grown at 1100 ºC; (ii) Then a SiO_2 (400 nm in thickness)/ Si_3N_4 (600 nm in thickness) membrane was successively deposited on each side of the silicon substrate by low pressure chemical vapor deposition (LPCVD) at 800 ºC; (iii) A nanolayer Al_2O_3 with a thickness of 10 nm was deposited by atomic layer deposition (ALD) and patterned by ion-beam etching; (iv) The Pt/Ti electrodes (10 μm wide and 10 μm separated) and bonding pads were patterned by lift-off process with the adhesive Al_2O_3 layer buried beneath Pt; (v) Then the SiO_2/Si_3N_4 membrane was selectively etched by Ion-beam to

form front etching windows and the membrane was released in a solution of TMAH (25 wt.%) at 80 ºC. So far, the microheater was prepared. (vi) Then a SiO_2 (600 nm in thickness) layer, a insulating layer, was deposited on it by plasma enhanced chemical vapor deposition (PECVD); (vii) the Pt/Au interdigital electrodes (10 μm wide and 10 μm spacing, 200 nm in thickness) and leading wires were patterned by lift-off process. (viii) Positive photolithography was used to define the corrosion windows for releasing the heating membrane area and the support cantilever; (ix) under the protection of the photoresist, the exposed silicon oxide and silicon nitride composite membrane were etched completely using reactive ion etching (RIE); (x) Silicon substrate was etched through the release windows using KOH etching solution, forming the inverted trapezoidal insulation cavity. By now, the IDEs-microheater MEMS-based chip was fabricated.

2. Mass-production illustration

By transferring the solution-dipped self-organized PS colloidal template onto a MEMS-based IDEs-microheater chip equipped wafer, we can easily realize the mass production of such gas sensors. Briefly, the area of the chip is about 9 mm^2 and the monolayer PS colloidal template can be prepared to be in 4 inch Si wafer area (see Figure S1). As we know, the IDEs-microheater chips can be manufactured in one wafer in batches by MEMS technology. It means that we can produce about 900 gas-sensing devices in one batch by transferring a solution-dipped wafer-scaled template onto the similarly-sized many chips outfitted wafer, as illustrated in Figure S2.

Figure S1. Z. Dai et al.

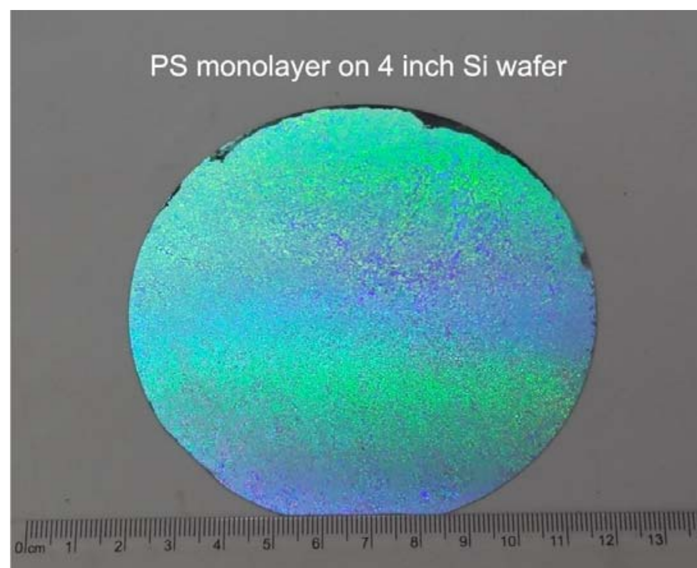

Figure S1. The monolayer PS colloidal template in 4 inch Si wafer area by an air/water interfacial self-assembly.

Figure S2. Z. Dai et al.

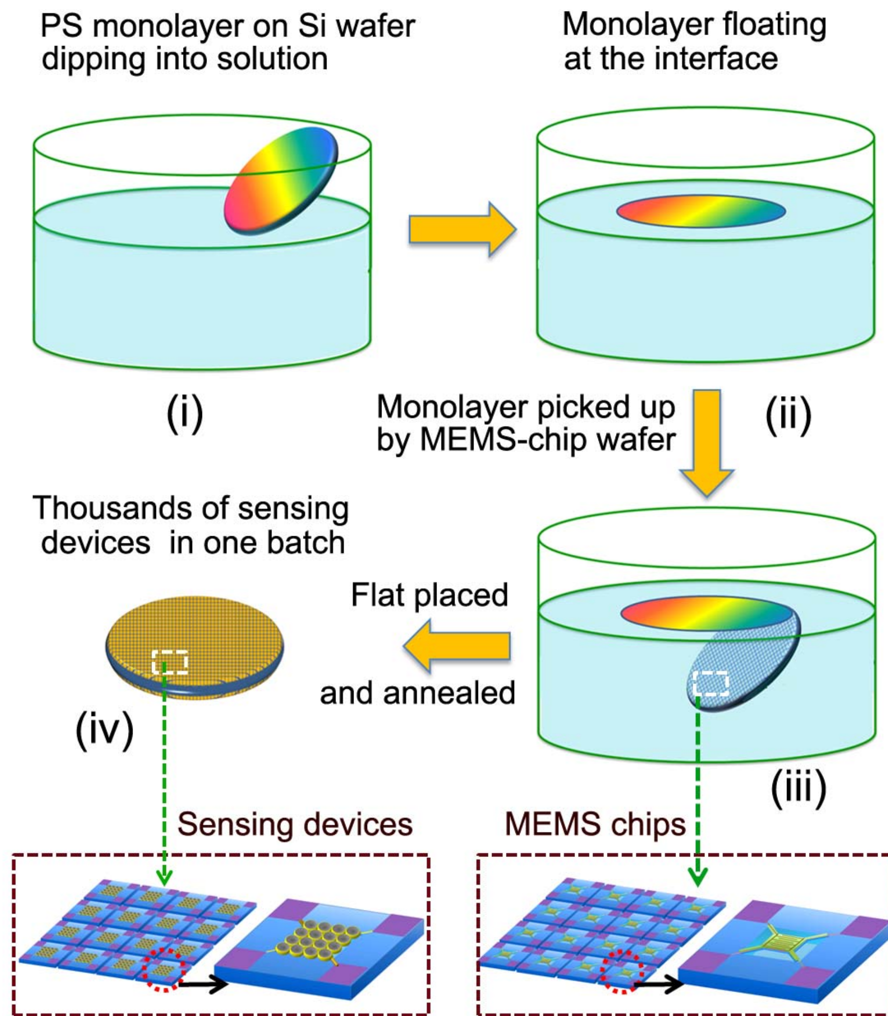

Figure S2. Schematic illustrations of the mass-produced sensors processing steps used to in-situ fabricate SnO_2 ordered porous film on an encapsulated MEMS chip equipped wafer.

Figure S3. Z. Dai et al.

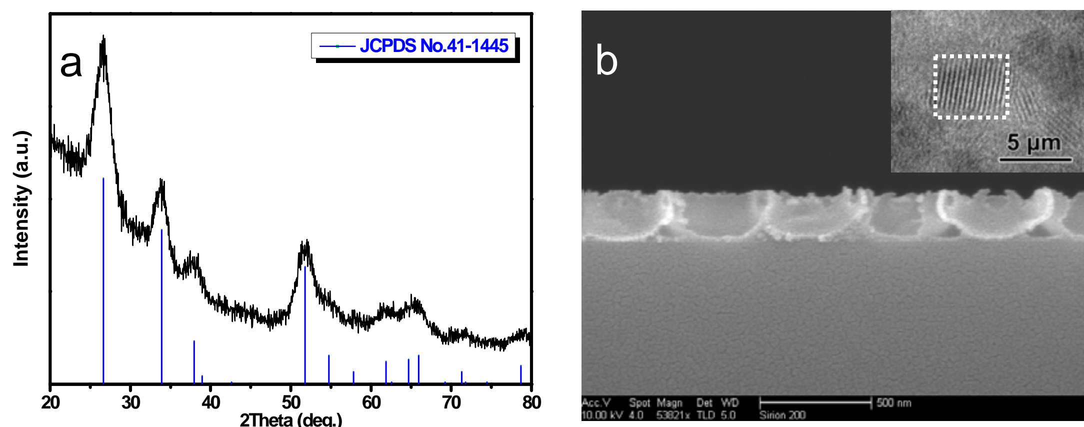

Figure S3. The phase analysis and morphology of the SnO_2 ordered porous film. (a) The XRD spectrum and (b) cross-sectional SEM image of the SnO_2 ordered porous film. The inset in (b) is the TEM image of the SnO_2 ordered porous film.

3. FEM simulation of temperature distribution on the sandwich chip

As mentioned before, a main goal in developing gas sensors is a homogenous temperature distribution on the active area. Since many semiconductor materials have strong temperature-dependent sensitivity and cross-sensitivity, temperature gradient on the active area should be as small as possible. Finite Element Method (FEM) simulations have been done by using the electro-thermo-mechanical simulations of commercial analysis software Coventor. Simulations have been performed assuming the following boundary conditions: (a) the temperature on the back side of the die is constant and set as room temperature 25 ^{o}C; (b) on the upper and lower surfaces of the membrane, heat is dissipated through convection and radiation; (c) electric voltages are applied on the pads of the Pt heater. Some parameters of thin films are different from those in bulk materials. The parameters used in our simulations are listed in Table SI.

Figure S4a shows the temperature distribution illustration of our microhotplate by FEM simulations under an electrical power of 34 mW. Temperature gradient on the supporting beams is high, which means that a lot of heat flows through the beams from the center heated membrane to the substrate. Letting x and L respectively as the distance from begin point to any point and the endpoint of the microheater (see Figure S4a), Figure S4b displays the temperature (^{o}C) distribution at different location of the chip. The active area (the central red square in Figure S4a) achieves a homogenous temperature distribution with an average temperature gradient of 0.2 ^{o}C/μm.

Figure S4. Z. Dai et al.

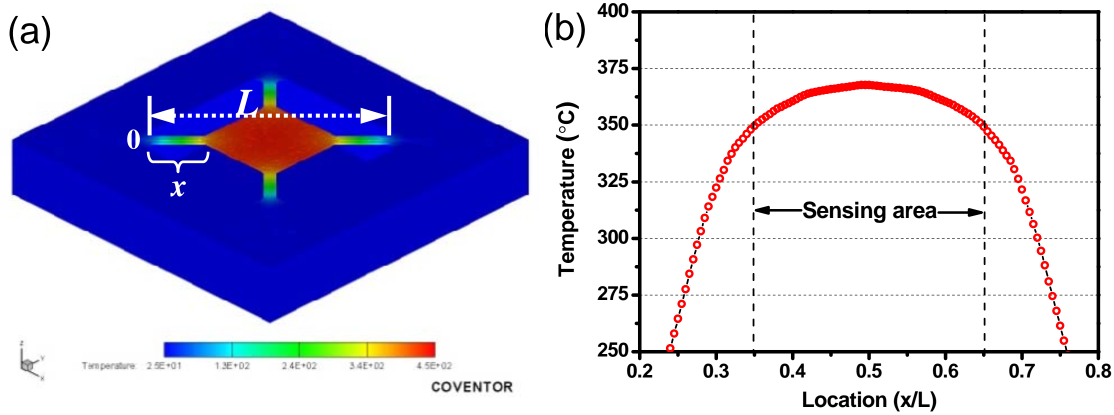

Figure S4. Electro-thermal analysis results at 34 mW heating power. (a) Temperature distribution illustration, (b) temperature (in degrees Celsius) distribution at different location of the chip by an electrothermomechanical simulations of analysis software Coventor.

Table SI. Parameters used in the FEM simulation

Materials	Thermal conductivity (W/mK)	Thermal expansion (1/K)	Density (Kg/m^3)	Heat capacity (J/kgK)
Pt	73	8.9×10^{-6}	2.15×10^{4}	130
SiNx	22	2.33×10^{-6}	3.1×10^{4}	700
SiO2	1.4	0.55×10^{-6}	2.2×10^{3}	730
Si	157	2.33×10^{-6}	2.32×10^{3}	700
air	0.026	-	1.16	1000

Figure S5. Z. Dai et al.

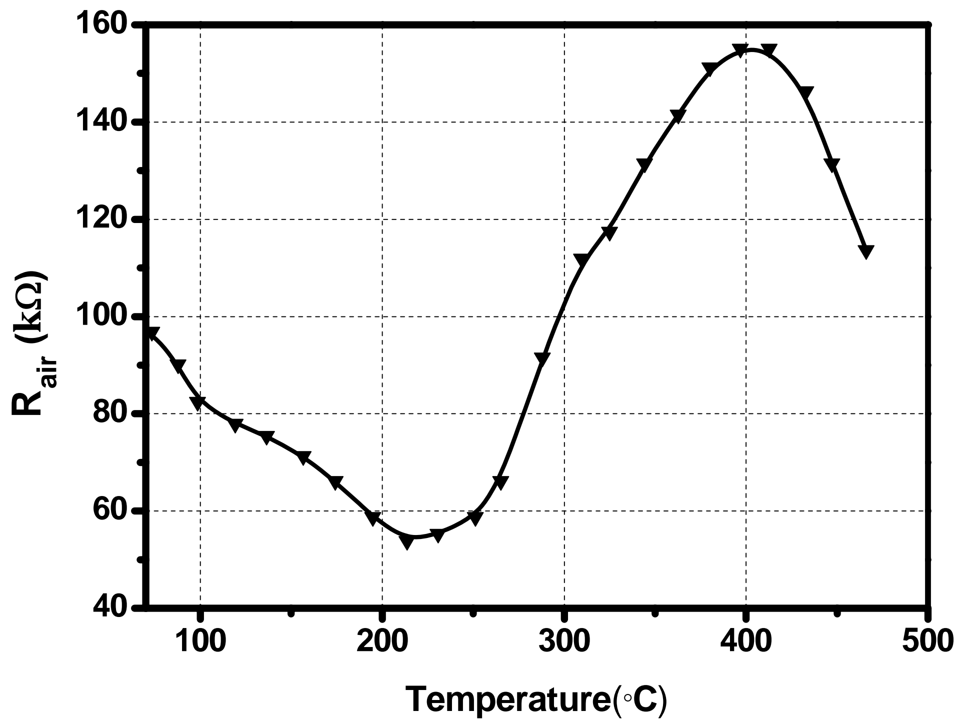

Figure S5. The resistance of the sensing thin film of the device in the air as a function of working temperature.

4. Instructions of the sensing process in a static measurement

First, the gas was injected into the operational chamber by a gas injector. Then, two symmetrically distributed high-speed rotating (300 rpm) fans can rapidly mix the analyte homogenously with the background air in the chamber (within 0.1s). To avoid an overhigh partial concentration (surrounding sensor) after injecting, a baffle plate design is introduced with the aim to keep the concentration surrounding sensor uniform. The interaction between sensors with target gas brings the change of the conductance which is recorded by a data acquisition (DAQ) instrument. Finally, the upper lid of the chamber is opened for the sensor recovery.

Figure S6. Z. Dai et al.

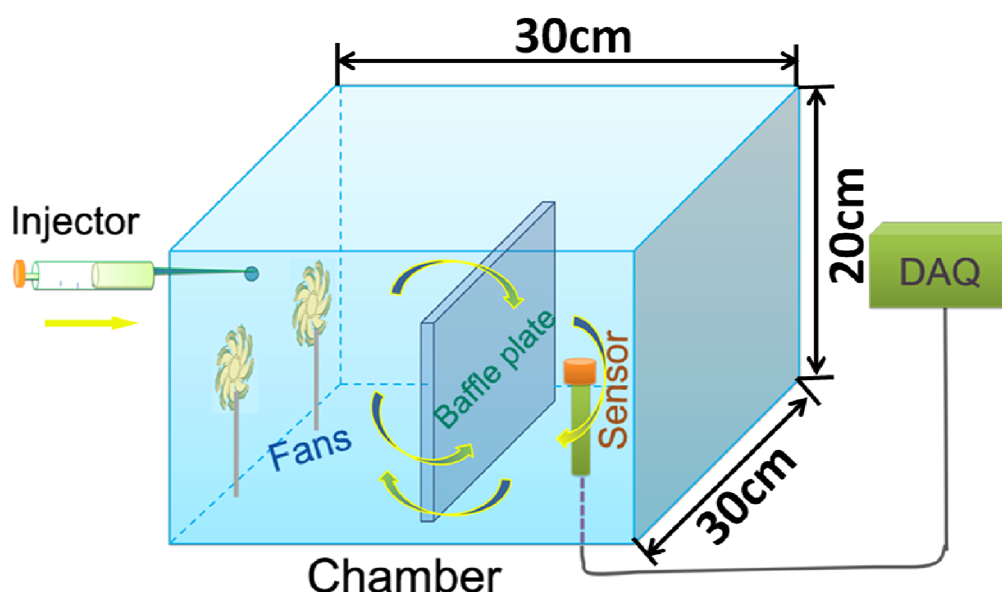

Figure S6. A schematic illustration of the gas sensing process in a static testing system.

Figure S7. Z. Dai et al.

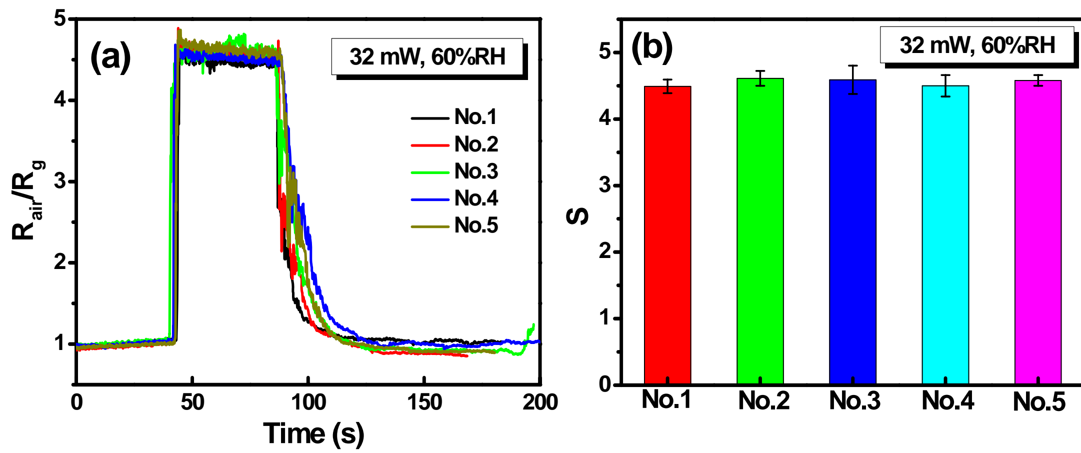

Figure S7. The repeatability of as-fabricated gas sensors. (a) EtOH-sensing (5 ppm) responses of five MEMS-based sensors fabricated by the same procedure under 350 ^{o}C (32 mW on microheater), 60%RH. (b) Bar graph summarizing the sensing signal change of such sensors of (a).

Figure S8. Z. Dai et al.

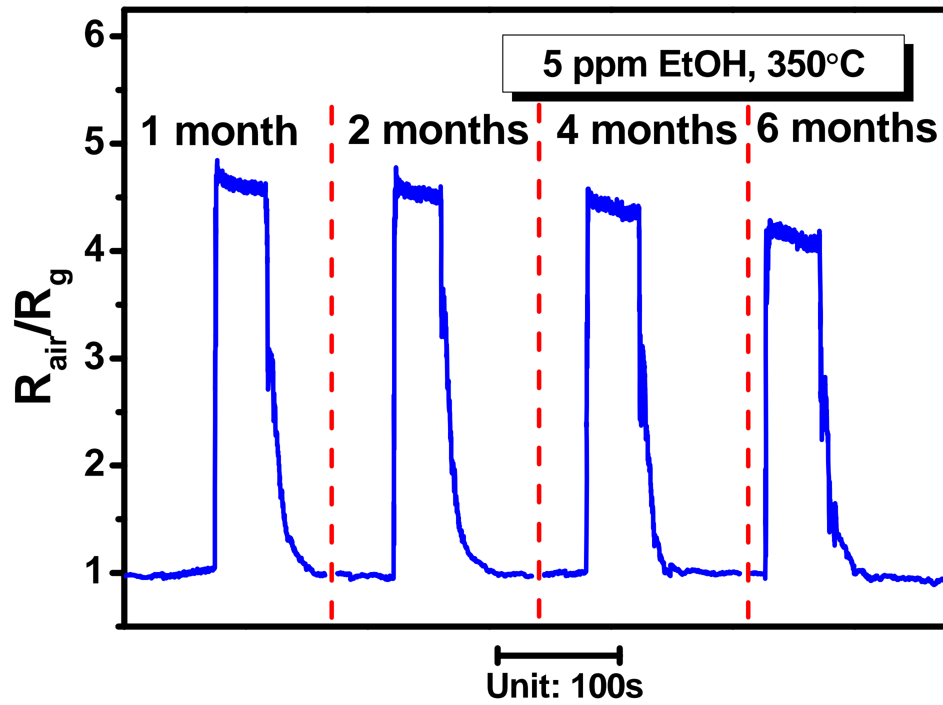

Figure S8. The 1, 2, 4 and 6 months-later sensing responses of the sensor to 5 ppm EtOH under 350 °C and 60%RH, respectively.

Figure S9. Z. Dai et al.

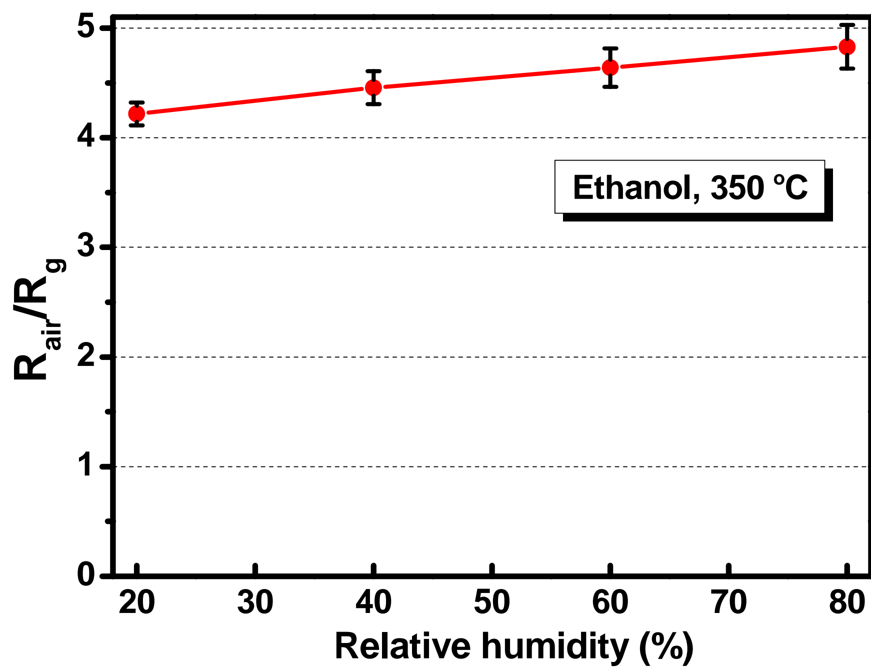

Figure S9. The EtOH-sensing (5 ppm, 350 ^{o}C) responses under different relative humidity ambients.

Figure S10. Z. Dai et al.

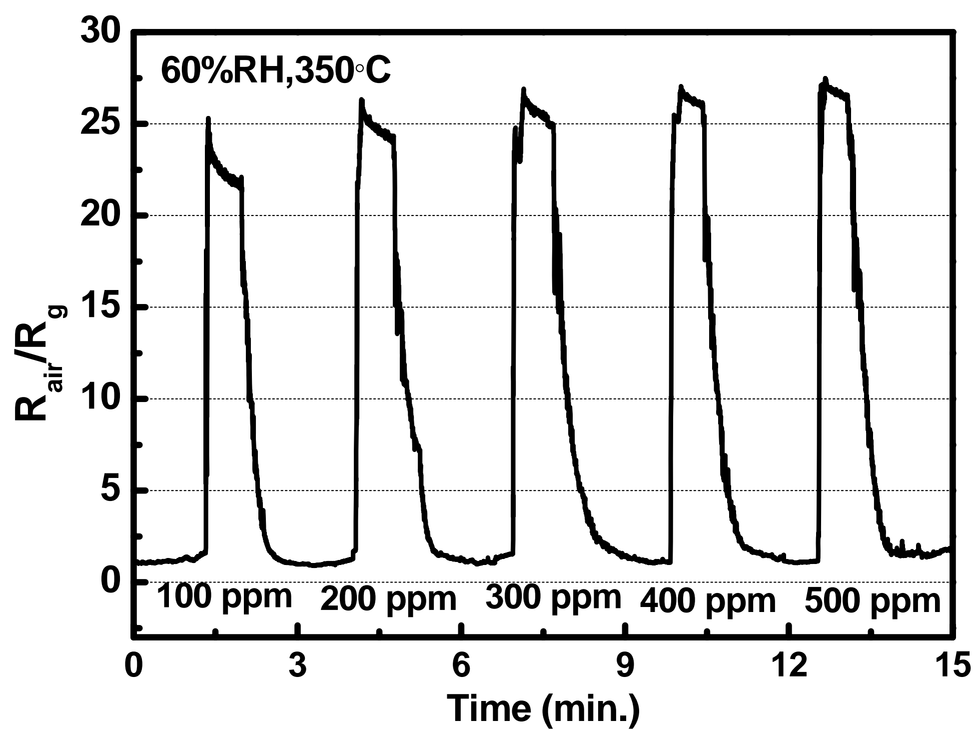

Figure S10. The real-time sensing response of the SnO_2 sensor to 100~500 ppm EtOH under 350 °C and 60%RH.